

TCP Reno over Adaptive CSMA

Wei Chen*, Yue Wang[†], Minghua Chen*, and Soung Chang Liew*

*Dept. of Information Engineering, The Chinese University of Hong Kong,

[†]School of Information, Central University of Finance and Economics

*{cw008, minghua, soung}@ie.cuhk.edu.hk, [†]yue.wang@cufe.edu.cn

Abstract—An interesting distributed adaptive CSMA MAC protocol, called adaptive CSMA, was proposed recently to schedule any strictly feasible achievable rates inside the capacity region. Of particular interest is the fact that the adaptive CSMA can achieve a system utility arbitrarily close to that is achievable under a central scheduler. However, a specially designed transport-layer rate controller is needed for this result. An outstanding question is whether the widely-installed TCP Reno is compatible with adaptive CSMA and can achieve the same result. The answer to this question will determine how close to practical deployment adaptive CSMA is. Our answer is yes and no. First, we observe that running TCP Reno directly over adaptive CSMA results in severe starvation problems. Effectively, its performance is no better than that of TCP Reno over legacy CSMA (IEEE 802.11), and the potentials of adaptive CSMA cannot be realized. Fortunately, we find that multi-connection TCP Reno over adaptive CSMA with active queue management can materialize the advantages of adaptive CSMA. NS-2 simulations demonstrate that our solution can alleviate starvation and achieve fair and efficient rate allocation. Multi-connection TCP can be implemented at either application or transport layer. Application-layer implementation requires no kernel modification, making the solution readily deployable in networks running adaptive CSMA.

I. INTRODUCTION

The Carrier Sense Multiple Access (CSMA) protocol is widely used in local-area networks, including Wi-Fi. As the deployment of Wi-Fi spreads, it is now common to find multiple co-located Wi-Fi networks with partially overlapping coverage. In such networks, each link can only sense a subset of other links, and characterizing the link throughput achievable by CSMA is challenging.

Refs. [1] and [2] show that the saturated link throughput achieved by CSMA can be studied via a time-reversible Markov chain and can be expressed in a product form. Further, authors in [2] showed that the product form results are insensitive to the packet length and back-off time distributions given the ratio of their means.

Based on these results on the CSMA link throughput, Jiang and Walrand [3], and later others [4]–[7], present a distributed adaptive CSMA (A-CSMA) scheme that can achieve desired link throughput according to some system utility objective. It is shown that the distributed A-CSMA scheme can achieve almost the entire capacity region that can be achieved under a central scheduler. Given its attractiveness and impenetrability [8], an outstanding question is how close A-CSMA is to practical deployment. As originally studied in [3], specially designed transport-layer rate controllers were required to inter-work with A-CSMA.

In view of the large installed base of TCP Reno, a question is whether TCP Reno over A-CSMA works well. We answer this question in this paper and make the following contributions:

- We observe that running TCP Reno directly over A-CSMA results in severe starvation problems. Effectively, its performance is no better than that of TCP Reno over legacy CSMA (IEEE 802.11) [1] [2] [9] [10]. Our analysis indicates that the root cause is that TCP Reno over A-CSMA results in system instability.
- We propose a multi-connection TCP Reno solution to inter-work with A-CSMA in a compatible manner. Although multi-connection TCP has been explored before in the context of video transmission over cellular and wired networks [11], [12], this paper applies it to solve starvation problem in TCP Reno over A-CSMA. Our solution is provably optimal under the Network Utility Maximization (NUM) framework. Specifically, by adjusting the number of TCP Reno connections for each session, any system utility can be realized. NS-2 simulations demonstrate that this solution can address starvation problems and achieve fair and efficient rate allocation. The scheme is applicable to single-hop wireless networks, wired networks as well as multihop networks with wired and wireless links.
- Our multi-connection TCP Reno scheme can be implemented at either the transport layer or the application layer. Application-layer implementation requires no kernel modification to TCP Reno, and the solution can be readily deployed over networks with A-CSMA.

The rest of the paper is organized as follows. We present related work in Section II, and the network model in Section III. We illustrate the starvation of TCP Reno A-CSMA in Section IV. We then propose our solution in the Section V, and evaluate its performance through NS-2 simulations in Section VI. Finally, Section VII concludes our paper.

II. RELATED WORK

Rate control (i.e., congestion control) is important for data transmission over both wired and wireless networks. The widely deployed rate control scheme is TCP Reno. To put our study in context, we classify the possible solutions into four classes, as shown in Table I, where we refer to CSMA/CA scheme used in today's Wi-Fi as legacy CSMA (L-CSMA).

Class 1 solutions use TCP Reno over L-CSMA. There have been extensive work studying the fairness problem of this scheme [1] [2]. They reveal that TCP Reno over L-CSMA

results in severe starvation problem. The main reason is that L-CSMA is not an efficient scheduling algorithm and it can only schedule a fraction of the capacity region.

TABLE I
RATE CONTROL AND SCHEDULING SOLUTION CLASSES

	L-CSMA	modified-MAC
TCP Reno	class 1	class 2
modified TCP	class 3	class 4

Class 3 solutions, for instance [9] [10], do not make any changes to the widely used IEEE802.11 MAC. In contrast, they limit the design space to within the scope of transport layer. In [9], the authors propose an AIMD-based rate control protocol called WCP Wireless Control Protocol (WCP) to address the efficient and fair rate allocation over L-CSMA networks. WCP halves the rates of other flows if they are within interference range of the congested link. Hence, queues of other fast transmitting links are driven to empty, giving the congested link opportunity to transmit. However, WCP requires message passing among the interfered links. Meanwhile, each link must monitor the Round-trip time (RTT) of every flow that traverses it. EWCCP [10] is designed to be proportional-fair by periodically broadcasting the average queue information to coordinate among interference links. These periodical broadcasted message consumes the precious wireless bandwidth.

There have been many efforts belonging to class 4. Cross-layer designs based on new TCP and new MAC are adopted [3]–[6], [13], [14]. Cross-layer designs can improve the overall system performance and make interaction between layers more transparent, but raise the hurdle to practical deployment.

Our solution belongs to class 2. First, it is a layered approach rather than a cross-layer one, reducing the implementation difficulty. Second, since TCP Reno is widely installed in practice, to make a network function well, it is preferable to avoid modifying TCP Reno.

Our solution is based on multiple connection TCP Reno. There has been work on using multiple connections to transfer data. For example, multiple TFRC connections for streaming video [15] and multiple TCP Reno connections for data and multimedia streaming [11], [12] have been discussed. These works focus on wired networks and wireless cellular networks. In contrast, our work focuses on CSMA networks and therefore solves a different set of challenges, including the spatial wireless inference that was not considered in [11], [12], [15].

Our solution utilizes active queue management (AQM) in the MAC. AQM techniques have been proposed to both alleviate congestion control problems [16] as well as to implement the provisioning of quality of service [17]. The classical example of an AQM policy is RED [16]. In our study, however, we apply a different AQM policy: the packet dropping probability is proportional to queue length. In our work, by applying this AQM, our scheme converges to the optimal solution.

III. PROBLEM SETTINGS

In this section, we provide problem settings and necessary background on A-CSMA and TCP Reno. We model a CSMA wireless network by a graph $G = (V, E)$, where V is the set of nodes (i.e., wireless transmitters and receivers) and E is the set of links. We consider the scenario where multiple users communicate over the wireless network. Each user is associated with a flow over a pre-defined route between a source and a destination. The key notations used in this paper are listed in Table II. We use bold symbols to denote vectors and matrices of these quantities, e.g., $\mathbf{x} = [x_s, s \in S]$.

TABLE II
KEY NOTATION

Notation	Definition
V	the set of nodes
E	the set of links
S	the set of source-destination pairs
x_s	rate of flow s
T_s	round trip time of flow s
n_s	number of connection on flow s
y_l	average rate of link l
τ_i	time portion of independent set i
r_l	transmission aggressiveness (TA) of link l
p_l	price of link l
$l \in i$	link l belongs to independent set i
$l \in s$	flow s passes through link l
\mathcal{I}	the set of independent sets

In CSMA wireless networks, transmitter applies a carrier-sensing mechanism to prevent collisions. In particular, a transmitter listens for an RF carrier before sending its data. If a carrier is sensed, the transmitter defers its transmission attempt, enters a countdown process in which it waits for a random amount of time before making another transmission attempt. As such, two links are allowed to transmit simultaneously only if the simultaneous transmissions are under the CSMA carrier-sensing operations.

If not properly designed, simultaneous transmissions allowed by the carrier-sensing operations may still interfere with each other, resulting in the hidden-node problem [18]. Hidden-node-free CSMA network designs are attractive, because, importantly, their throughput analysis is tractable [1] [2]. In particular, the stationary distribution of the system state is in a product form that is fundamental to the design of adaptive CSMA [3]. As studied by [19], any CSMA wireless network can always be made to be hidden-node-free by setting the carrier sensing range properly.

In this paper, we study the problem of end-to-end rate control and link scheduling in hidden-node-free CSMA wireless networks.

A. Capacity Region of CSMA Wireless Networks

For CSMA wireless networks, we use the conflict graph approach in [20] to model the relationship of wireless link interference. We denote the conflict graph of G by $G_c = (V_c, E_c)$. The vertices of G_c correspond to links E in the communication graph G , i.e., $V_c = E$. An edge between two vertices means that the two corresponding links can carrier-sensing each other. An independent set corresponds to a feasible schedule which

is a set of links in the communication graph that can be active simultaneously.

Let \mathcal{I} denote the set of all independent sets, τ_i denote the fraction of time the system is in schedule $i \in \mathcal{I}$. Assuming that all links have unit capacity, the capacity region of link rate is given by

$$\Pi = \{\mathbf{y} \geq 0 | \forall l, y_l \leq \sum_{i:l \in i} \tau_i, \sum_{i \in \mathcal{I}} \tau_i = 1, \tau \geq 0\}. \quad (1)$$

Note that finding all the independent sets is NP-hard [21]. Consequently, characterizing the capacity region in (1) is thus very challenging, leaving alone attaining it in practice.

B. Throughput-optimality of A-CSMA

Refs. [22], [1] and [2] show that the link scheduling in CSMA networks can be studied via a Markov chain, in which the states are all independent sets. In this model, the transmitter of link l counts down an exponentially distributed random period of time with mean $\exp(-\beta r_l)$ before transmission. When the link l starts a transmission, it keeps the channel for an exponentially distributed period of time with mean one¹. This CSMA Markov chain converges to its product form stationary distribution, which is given by

$$p(i, \mathbf{r}) = \frac{\exp(\sum_{l \in i} \beta r_l)}{\sum_{i' \in \mathcal{I}} \exp(\sum_{l \in i'} \beta r_l)}, \quad \forall i \in \mathcal{I}, \quad (2)$$

where β is the a positive constant. The average portion of time link l is active, denoted by y_l , achieved in steady state is given by

$$y_l(\mathbf{r}) = \sum_{i:l \in i} p(i, \mathbf{r}) = \frac{\sum_{i:l \in i} \exp(\sum_{l \in i} \beta r_l)}{\sum_{i' \in \mathcal{I}} \exp(\sum_{l \in i'} \beta r_l)}, \quad \forall l \in E. \quad (3)$$

The authors in [3] introduce a fully distributed adaptive CSMA (A-CSMA) algorithm as follows:

Algorithm A-CSMA.

$$\dot{r}_l = \alpha [a'_l - d'_l]_r^+, \quad (4)$$

where a'_l and d'_l are the empirical average arrival rate and service rate of link l , α is constant step size and notationally,

$$[g(z)]_z^+ = \begin{cases} \max(g(z), 0), & \text{if } z \leq 0 \\ g(z), & \text{otherwise} \end{cases} \quad (5)$$

Theorem 1 ([3]). Assume arrival rate vector \mathbf{y}' is in interior of capacity region Π . Then with Algorithm A-CSMA, \mathbf{r} converges to \mathbf{r}^* , with probability one, where \mathbf{r}^* satisfies that $y'_l \leq y_l(\mathbf{r}^*)$.

Remark 1: it is not difficult to verify that r_l is proportional to its local queue length of link l . Therefore, A-CSMA scheduling Algorithm A-CSMA can be implemented in a fully distributed way. In A-CSMA, before transmitting, any link l sets up a random exponentially distributed counter with mean equal to $\exp(-\beta r_l)$. When link l obtains the channel, it transmits a packet with length which is exponentially distributed with mean equal to one. Note A-CSMA differs from L-CSMA in that the link's countdown timer is a function of its queue length, as a result, A-CSMA gives priority to links with heavy

¹Without loss of generality, we normalize the mean of transmission time to one.

loads. We remark that A-CSMA is simple to implement by slight modification to today's CSMA, and there have been efforts in doing so [8].

Remark 2: Theorem 1 shows that the product-form distribution $\mathbf{y}(\mathbf{r})$ achieved by A-CSMA is larger than any interior feasible rate vector. This means A-CSMA stabilizes the system for all feasible arrival rate vector, i.e., A-CSMA scheduling algorithm is throughput-optimal. Therefore, A-CSMA has superior performance as compared to L-CSMA.

For more details of A-CSMA, interested readers can refer to the work in [3]–[7].

C. TCP Reno Congestion Control Modeling

TCP Reno adjusts the flow rate by controlling the congestion window size W . During the congestion avoidance phase, TCP Reno increments its congestion window W by one every round trip time if no loss is observed. It halves its window whenever packet loss is detected.

In [23], the authors model this dynamic of the congestion avoidance phase of TCP Reno with the following dynamic equation:

$$\dot{x}_s = \frac{x_s^2}{2} \left(\frac{2}{T_s^2 x_s^2} - \sum_{l \in s} p_l \right) \quad (6)$$

where T_s is round-trip-time(RTT) of flow s , and p_l denotes the price (probability a packet will be dropped) of link l . When link l applies drop-tail queue,

$$p_l = \frac{(\sum_{s:l \in s} x_s - y_l)^+}{\sum_{s:l \in s} x_s}, \quad (7)$$

where y_l denotes average throughput of link l , and $[\cdot]^+$ denotes $\max(0, \cdot)$.

IV. TCP RENO OVER A-CSMA

As stated in the previous section, A-CSMA scheduling algorithm is throughput optimal and can be easily implemented by slightly modifying the existing L-CSMA [3]–[7]. Observing the large installed base of TCP Reno, a natural question to ask before actual deployment of A-CSMA network is how well TCP Reno can perform over A-CSMA networks.

In this section, we study the performance of TCP Reno directly running over A-CSMA network. Surprisingly, our simulation reveals that TCP Reno over A-CSMA suffers from starvation problem. In particular, it is no better than TCP Reno over L-CSMA network². By applying TCP Reno, the potential advantages of A-CSMA cannot be realized.

A. TCP Reno Starves over A-CSMA

We carry out NS-2 simulation to demonstrate the starvation problem of running TCP Reno directly over A-CSMA. The network topology is shown in Fig. 1(a). Each link carries a single TCP Reno connection. The simulation settings are as follows: 1) update step size and update interval for r are 0.05 and 2.0 respectively; 2) β : weight of entropy term is

²The starvation problem of TCP Reno over L-CSMA, has been extensively studied in previous work, such as [1], [2]. We give an example of starvation of TCP Reno over L-CSMA in Appendix A.

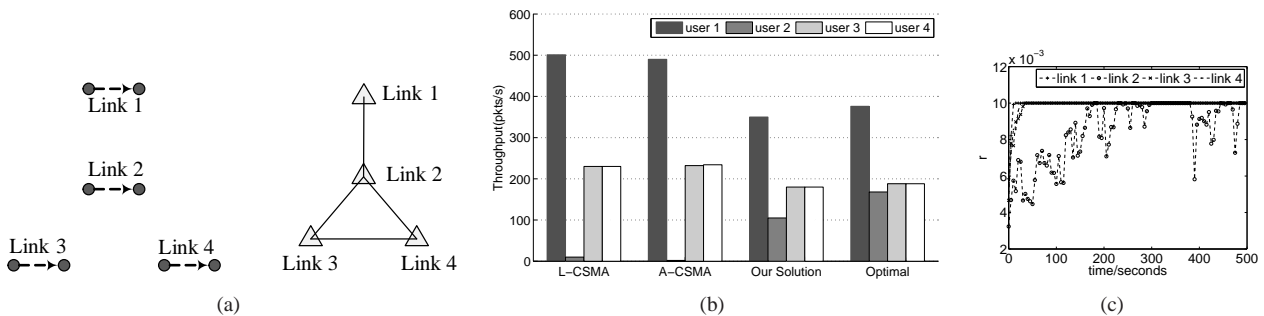


Fig. 1. (a) a wireless network of four links. Its conflict graph is shown on the right hand side. (b) throughput under 1) L-CSMA: NS-2 simulation of TCP Reno over L-CSMA, 2) A-CSMA: NS-2 simulation of TCP Reno over A-CSMA, 3) our solution: NS-2 simulation of multi-connection TCP Reno over A-CSMA with AQM, 4) optimal: optimal throughput computed from problem **MP**. (c) transmission aggressiveness under A-CSMA in NS-2 simulation.

800; 4) data rate of wireless networks is 11Mbps; 5) TCP payload is 1000 byte. To prevent the countdown from being too aggressive³, we set the upper bound for r to be $r_{\max} = 0.01$. We remark that our simulation results hold as long as βr_{\max} is bounded. To get a clear understanding, we only consider the forward link (the link that transmits TCP DATA) in the analysis by letting the backward link send back the TCP ACK with higher priority than forward link TCP DATA. To achieve this goal, we set the backward link with a fixed maximum transmission aggressiveness r_{\max} . Consequently, most of the packets are buffered in the queue of the forward links.

Fig. 1(c) shows the throughput achieved under TCP Reno over A-CSMA and that under TCP Reno over L-CSMA respectively. We can see that they have nearly the same performance. In both cases, user 2 has less throughput than other users does and therefore starves. These results show that TCP Reno over A-CSMA also suffers from severe starvation. Effectively, its performance is no better than that of TCP Reno over L-CSMA, and the potential of A-CSMA cannot be realized by running TCP Reno directly over it. Because of the large installed base of TCP Reno, many Internet services such as HTTP and FTP that relies on TCP will suffer over A-CSMA networks.

B. Observations and Explanations

The explanation of this starvation phenomenon is as follows. Initially all links have the same r and compete the channel with the same level of transmission aggressiveness. Under the link interference relationship, links 1, 3 and 4 will take turns to freeze link 2, and link 2 is not able to obtain its fair share. This is the same as the origin of the starvation problem of L-CSMA discussed in Appendix A. To avoid starvation, link 2 must be able to count down with larger transmission aggressiveness than other links, so as to compete more aggressively for the fair channel share against the other three (less aggressive) links.

However, with TCP Reno running over A-CSMA, link 2 actually obtains a smaller transmission aggressiveness than other links, exacerbating its starvation. We explain this as follows. TCP Reno increases its rate more slowly when it experiences larger RTT, and vice versa. Initially, link 2 suffers from freezing of its backoff countdown for longer time because

³If transmission aggressiveness are too large, $\exp(-\beta r_l)$ should be very tiny, this will result in zero countdown in digital system.

of the transmissions of its neighbors. Consequently, TCP Reno over link 2 experiences larger RTT and increases its congestion window more slowly than those over other links. In our example, the TCP congestion window size roughly equals to the buffer length, thus link 2's queue increases more slowly than those of other links. Since A-CSMA sets the transmission aggressiveness to be proportional to the queue length, link 2 ends up having the smallest transmission aggressiveness among all the four links. This explanation is verified by the simulation results on transmission aggressiveness in Fig. 1(c).

This is a positive feedback loop. Larger transmission aggressiveness will lead to shorter RTT. Shorter RTT makes TCP Reno increase its rate faster, thus the larger congestion window. Larger congestion window leads to longer queues, thus larger transmission aggressiveness. This loop continues until the transmission aggressiveness of all the links reach the same upper limit r_{\max} . With $r_l = r_{\max}$ for $l = 1, 2, 3, 4$, the performance of TCP Reno over A-CSMA falls back to the performance of TCP Reno over L-CSMA, and link 2 suffers starvation as discussed in Appendix A.

V. PROPOSED SOLUTION

In this section, we propose to use a layered approach of multi-connection TCP Reno over A-CSMA with AQM as a practical solution to achieve fairness. This solution is provably optimal under NUM framework. Interestingly, it can be extended to wired network and multihop networks with wired and wireless links without any change. In this solution, we stick to today's TCP Reno instead of designing a new TCP for the following reasons. First, many Internet services (e.g. HTTP, FTP) currently rely on the most widely-installed TCP Reno. Second, TCP Reno has been well-tested in the Internet scale. Last, compatibility concern seems challenging and not well-understood yet [24]. A new TCP needs to be carefully designed to be compatible with today's TCP Reno.

A. Proposed Solution: Multi-connection TCP Reno Scheme

We observe that TCP Reno interacts with A-CSMA through both RTT and packet loss rate. First, any loss based TCP will interact with the queue-based A-CSMA through packet loss rate. For the interaction to behave properly, we always need to employ AQM to calibrate the mapping between the link queue-length and the link loss rate. Second, it has been observed and

discussed in the previous section that the reason of the flow starvation is that it suffers long RTT, which is caused by the long MAC access delay. To remove TCP bias on RTT, one way is to open multiple number of connections proportional to the RTT that TCP experiences. In this way, TCP Reno with large RTT that will open more connections to compensate for the small congestion window of each connection. As a result, there are more outstanding packets filling in the queue of the link. This makes A-CSMA allocate more airtime to the link, reducing its MAC accessing delay of the link and thus the RTT of the flow.

Inspired by the above observations, we propose to use multi-connection TCP Reno to remove the RTT interaction between TCP Reno and A-CSMA, and use AQM to calibrate their packet loss interaction.

In our solution, every user s monitors the round trip time T_s , and opens $n_s = kT_s$ (where k is a constant) TCP Reno connections to remove the RTT bias. We remark that now the user rate x_s is the aggregate rate of n_s TCP Reno connections. We present the overall scheme as the following dynamic system:

$$\begin{cases} n_s = kT_s, \forall s \in \mathcal{S}; & (8) \\ \dot{x}_s = \frac{x_s^2}{2n_s} \left(\frac{2n_s^2}{T_s^2 x_s^2} - \sum_{l \in \mathcal{S}} r_l \right)_{x_s}^+, \forall s \in \mathcal{S}; & (9) \\ \dot{r}_l = \alpha \left[\sum_{s: l \in \mathcal{S}} x_s - \sum_{i: l \in \mathcal{I}} \tau_i(\mathbf{r}) \right]_{r_l}^+, \forall l \in \mathcal{L}, & (10) \end{cases}$$

where

$$\tau_i(\mathbf{r}) = \frac{\exp(\sum_{l \in \mathcal{I}} \beta r_l)}{\sum_{i' \in \mathcal{I}} \exp(\sum_{l \in \mathcal{I}} \beta r_l)}, \forall i \in \mathcal{I}. \quad (11)$$

We remark that how T_s is updated is irrelevant to our solution as we always compensate for its impact by opening n_s connections. The multi-connection TCP Reno dynamic equation can be expressed in the form of (9)⁴ [11] when the end-to-end price (e.g., packet loss rate) is $\sum_{l \in \mathcal{S}} r_l$. This link price can be fed back by packet loss based technique like Active Queue Management (AQM). In this paper, we adopt an AQM policy in which each link drops or ECN-marks packet with probability equal to r_l . We remark that the independent sets distribution satisfies (11) as long as each link applies CSMA mechanism and backoff with mean equal to $\exp(-\beta r_l)$. Dynamic equations (10) are exact to A-CSMA algorithm introduced in Section III-B and r_l is proportional to queue length.

The above dynamic system achieves certain system utility. With the time-scale separation assumption, it is stable and

⁴Recall that the single connection TCP Reno congestion window dynamic equation is,

$$\dot{W}_s = \frac{1}{T_s} - \frac{W_s^2}{2T_s} \left(\sum_{l \in \mathcal{S}} p_l \right), \quad (12)$$

where T_s is the round trip time and $\sum_{l \in \mathcal{S}} p_l$ is the end-to-end packet loss rate experienced by the TCP Reno. If flow s opens n_s number of TCP connection, the flow rate x_s can be expressed as

$$x_s = \frac{n_s W_s}{T_s}. \quad (13)$$

From (12) and (13), we now have

$$\dot{x}_s = \frac{x_s^2}{2n_s} \left(\frac{2n_s^2}{T_s^2 x_s^2} - \sum_{l \in \mathcal{S}} p_l \right). \quad (14)$$

converges to the unique equilibrium. We summarize the result as the following theorem.

Theorem 2. 1) *Equilibrium of dynamic system in (8)-(10) solves the following Network Utility Maximization problem⁵:*

$$\begin{aligned} \mathbf{MP}: \quad & \max_{\mathbf{x} \geq 0, \boldsymbol{\tau} \geq 0} \sum_s -\frac{1}{x_s} - \frac{1}{\beta} \sum_{i \in \mathcal{I}} \tau_i \log \tau_i \\ & \text{s.t.} \quad \sum_{s: l \in \mathcal{S}} x_s \leq \sum_{i: l \in \mathcal{I}} \tau_i, \quad \forall l \in \mathcal{E}, \quad (15) \\ & \sum_{i \in \mathcal{I}} \tau_i = 1, \quad (16) \end{aligned}$$

2) *With the time-scale separation, i.e., the A-CSMA Markov chain converges to its stationary distribution instantaneously, the dynamic system (8)-(10) globally asymptotically converges to the unique optimal solution of problem MP.*

Remark: at the equilibrium, the utility function $-\frac{1}{x_s}$ guarantee an α -fairness among users with $\alpha = 2$ [25]. One of its implications is that *no user will starve at the optimal solution at the equilibrium*. This provides theoretical justification that our proposed solution will effectively address the TCP-Reno over A-CSMA starvation problem. The proof of Theorem 2 1) is given in Appendix C.

Theoretically, under the fluid model analysis, the proof of convergence can still be established under some mild conditions on parameters. The ideas are very similar to those expounded in [26], [27]. We skip the proof here due to space limitation.

Without such time-scale separation assumption, the dynamic system turns into a stochastic dynamic system, where the link rate measured by link l does not satisfy equations (11). Under small step size and update interval, the resulted stochastic dynamic system is shown to converge to a bounded neighborhood of the same optimal solutions with probability one [7], [27].

We validate the convergence of the algorithm in packet-level simulations later in Section VI.

B. Implementation

Inspired by the observations from the dynamic systems in (8)-(10). We can solve the problem by running multi-connection TCP Reno over A-CSMA with AQM. We stress multi-connection is important in our solution in that it removes the RTT interaction with A-CSMA. Without removing such RTT bias on RTT, TCP Reno over A-CSMA with AQM also results in starvation problem. Interested readers can refer to our Appendix B for detailed results and analysis.

The multi-connection layer can be implemented in two ways, without modification to the transport layer. One method is to insert an intermediate layer between the application layer and transport layer, called Multi-connection API. It provides the universal API to the application layer, and functions to maintain kT_s TCP Reno connections from monitored RTT.

⁵This formulation is similar to rate control over TDMA network except that there is an additional entropy term in the objective function. As shown in [3], [7], this leads to distributed implementation by using A-CSMA.

This solution requires no modification to TCP/IP stack and is compatible with today's applications (like FTP, HTTP, etc.).

The other implementation method is to rewrite the applications. The application keeps monitoring RTT and opens multiple sockets. To obtain the RTT, we can simply set up a UDP connection to measure the RTT [11], [15].

We prefer the first implementation in which we insert an multi-connection API in between. This implementation does not require any modification to today's applications and hence simplifies programming. From the structure of the dynamic system in (8)-(10), it can be implemented in a layered manner as follows, with the diagram shown in Fig 2:

- in the MAC layer, we run A-CSMA to schedule the link transmissions. This is directly obtained from dynamic equations (10). A-CSMA maintains transmission aggressiveness vector \mathbf{r} to be proportional to the lengths of links' queue.
- we run AQM at each link that drops or marks packets with a probability proportional to \mathbf{r} , and thus proportional to the queue lengths. In this way, the prices of using individual links can be fed back to end users via packet losses or ECN marks. We remark that AQM is required if we want to run loss based TCP (e.g. Reno) over A-CSMA.
- in the transport layer: we perform rate control based on sum of the prices of individual links, which is fed back in a form of packet losses or ECN marks. This result is directly obtained from equations (9). When loss ratio of link l is r_l , the total loss ratio that TCP Reno sees is $1 - \prod_{l \in \mathcal{S}} (1 - r_l) \approx \sum_{l \in \mathcal{S}} r_l$, when r_l is small.
- multi-connection layer, we maintain $n_s = kT_s$ connections to remove the RTT bias.

We remark that AQM is minimally required in order to run loss-based TCP (e.g. TCP Reno) over A-CSMA. The pseudo code of A-CSMA with AQM is shown in Alg. 1.

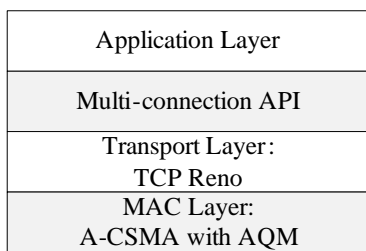


Fig. 2. Scheme Diagram

In practice, user s can only open an integer number of connections. By setting $n_s = \text{int}(kT_s)$, user s can react to the change in T_s in fine granularity if k is large, and in coarse granularity for small k . While large k is preferred in theory, in practice user s may need to maintain a large number of connections if k is too large. Large k also make the n_s adjustment more responsive to the changes in T_s , so it induces more overhead due to frequently opening and closing TCP Reno connections.

Packet loss ratio should be far less than one, otherwise it will waste considerable bandwidth for dropping large number

Algorithm 1 : Pseudo code of A-CSMA with AQM.

```

1: // Updating the transmission aggressiveness:
2: if at the end of time unit  $t - 1$  then
3:   Transmission aggressiveness  $r_l \leftarrow \alpha \cdot Q_l(t - 1)$ .
4: end if
5: // Setting the backoff window:
6: if before transmitting a packet with size  $PKT$  then
7:   Sets the backoff window following exponential distribution with mean equal to  $PKT * \exp(-\beta r_l)$ .
8: end if
9: // Adjusting the queue length:
10: if a packet is served then
11:   Queue length  $Q_l(t) \leftarrow \max(Q_l(t) - 1, 0)$ .
12: end if
13: if a new packet is inserted into queue then
14:   (a) Discards tail packet with probability  $\min(r_l, 1)$ .
15:   (b)  $Q_l(t) \leftarrow Q_l(t) + 1$ .
16: end if
17: if no packet to serve in the queue then
18:   Generates a dummy packet.
19: end if

```

of packets. Besides, the total loss ratio $1 - \prod_{l \in \mathcal{S}} (1 - r_l)$ does not hold when r_l is large. We can scale r_l so as to make it much smaller than one.

C. Discussion

We discuss the following two questions in this subsection: 1) By using multi-connection TCP Reno, can we achieve arbitrary utility function? 2) Is our solution applicable to wired network as well as multihop networks with wired and wireless links?

1) *Achieve Arbitrary Utility*: For the first question, our answer is yes. Let $U_s(x_s)$ be arbitrary utility function of problem **MP**. Consider our solution in (8)-(10) but replacing the updating equation of n_s as follows:

$$n_s = k \sqrt{\frac{U'_s(x_s) T_s^2 x_s^2}{2}}. \quad (17)$$

It is not difficult to verify that the equilibrium of the modified solution solves problem **MP** with the specified utility function $U_s(x_s)$.

In particular, our proposed solution can be understood as a special case of the above approach with the specified utility function being $U_s(x_s) = -\frac{1}{x_s}$.

2) *Extension to Networks with Both Wired and Wireless links*: Our answer to the second question is also yes. We consider a multihop network composed of wired and wireless links. Let l denote the wireless link and w denote the wired link. Our dynamic system to solve the extension problem of networks composed of wired and wireless links is as follows:

$$\begin{cases} n_s = kT_s, \forall s \in \mathcal{S}; & (18) \\ \dot{x}_s = \frac{x_s^2}{2n_s} \left(\frac{2n_s^2}{T_s^2 x_s^2} - \sum_{l \in \mathcal{S}} r_l - \sum_{w \in \mathcal{S}} p_w \right)_{x_s}^+, \forall s \in \mathcal{S}; & (19) \\ \dot{r}_l = \alpha \left[\sum_{s: l \in \mathcal{S}} x_s - \sum_{i: l \in \mathcal{I}} \tau_i(\mathbf{r}) \right]_{r_l}^+, \forall l \in \mathcal{E}', & (20) \end{cases}$$

where

$$\tau_i(\mathbf{r}) = \frac{\exp(\sum_{l \in i} \beta r_l)}{\sum_{l' \in \mathcal{I}} \exp(\sum_{l \in l'} \beta r_l)}, \quad \forall i \in \mathcal{I}. \quad (21)$$

$$p_w = \frac{(\sum_{s': w \in s'} x_{s'} - C_w)^+}{\sum_{s': w \in s'} x_{s'}}, \quad \forall w \in E_w, \quad (22)$$

and E_w denotes the set of wired links, E_l denotes the set of wireless links, C_w stands for the capacity of wired link w , and p_w is the packet loss ratio of wired link (when it applies drop-tail queue).

Theorem 3. *Equilibrium of dynamic system in (18)-(20) solves the following Network Utility Maximization problem:*

$$\begin{aligned} EP: \quad \max \quad & \sum_s -\frac{1}{x_s} - \frac{1}{\beta} \sum_{i \in \mathcal{I}} \tau_i \log \tau_i \\ & - \sum_{w \in E_w} \int_0^{\sum_{s': w \in s'} x_{s'}} \frac{(y - C_w)^+}{y} dy \end{aligned} \quad (23)$$

$$s.t. \quad \sum_{s: l \in s} x_s \leq \sum_{i: l \in i} \tau_i, \quad \forall l \in E', \quad (24)$$

$$\sum_{i \in \mathcal{I}} \tau_i = 1, \quad (25)$$

$$\mathbf{x} \geq 0, \tau \geq 0, \quad (26)$$

where the utility function is $U_s(x_s) = -\frac{1}{x_s}$, $\forall s \in \mathcal{S}$ and $\int_0^{\sum_{s': w \in s'} x_{s'}} \frac{(y - C_w)^+}{y} dy$ is the penalty function which penalizes the arrival rate for exceeding the wired link capacity c_w .

This theorem can be proved using similar method of the proof of Theorem 2.

From the above extension dynamic system, we have the following observations: 1) in MAC layer, wireless links perform A-CSMA with AQM; 2) link dropping ratio at wireless link is exact equal to packet dropping probability at today's routers (with drop-tail queue). Therefore, our solution discussed in Section V-B can be directly extended to networks with wired and wireless links without modification to any network components.

VI. SIMULATIONS

We evaluate the performance of multi-connection TCP Reno over A-CSMA stated in Section V-A with NS-2 simulation. A-CSMA with AQM is implemented following the description of Algorithm 1 by modifying the IEEE 802.11 module. Unless specified otherwise, the simulation parameters are the same. All simulations are conducted with zero channel losses, so as to give us a clear observation. By default, 1) k : the coefficient for n_s , is 10; 2) update step size α and update interval for r are 0.05 and 2.0second, respectively; 3) the weight of entropy term $\beta = 2000$; 4) data rate is 11Mbps; 5) carrier sensing range and transmission range are 800m and 250m respectively to avoid hidden-node problem. We do not wish to vary the number of TCP Reno connection too dynamically. In the simulation we update the connection number every 5 seconds. In the following subsections, we will investigate our solution under three different scenarios: single-hop networks, multihop pure wireless networks and multihop networks with wireless links and wired links.

A. Single-hop Networks Scenario

In this part, we consider single-hop wireless link data transmission. We run TCP Reno over L-CSMA, TCP Reno over A-CSMA, and Multi-connection TCP Reno over A-CSMA with AQM on the given topologies. We measure the throughput achieved by each user in different schemes, and compare these throughput with the optimal value. The optimal throughput is computed by solving the utility maximization problem **MP**.

To understand the performance of multi-connection TCP Reno over A-CSMA with AQM, we examine three different topologies with conflict graphs shown in Fig. 3. All topologies consist of four links, with each link carrying a single user data flow. Each of these three topologies has the starvation problem when TCP Reno is running over L-CSMA networks, which has been studied in [2]. In topology a, which has been studied in previous sections, TCP flow running over link 2 starves. In topology b, link 1 starves and links 2, 3 and 4 obtain the whole portion of channel access. In topology c, links 2 and 3 starve, link 1 and link 4 get the half of the channel bandwidth. This result can also be seen from the NS-2 simulation result in Fig. 4.

We plot the throughput obtained by different schemes in Fig. 4. Our multi-connection TCP Reno scheme guarantees the contending users in wireless network fairly share the channel. We define utility gap $\Delta U = \sum_s (U(x_s) - U(x_s^*))$ as the difference between the system achieves and the optimal utility. The closer ΔU to zero, the closer the system to the optimal. We give the utility gap under different scheme in all topologies in Table. III. This proves that our solution is capable of realizing the benefit of A-CSMA networks and achieving fair rate allocation in wireless network without any modification to TCP/IP stack in a fully distributed way. We observe that there is an optimality gap between our solution and optimal. Count down wastes some bandwidth, therefore, the performance is surely lower than optimal. The other reason is sharp oscillations of RTT. In our analysis, we assume that RTT is equal to average queuing delay plus propagation delay, which changes sharply in practice.

TABLE III
UTILITY GAP ΔU UNDER DIFFERENT SCHEMES

	Topo. a	Topo. b	Topo. c	Topo. d	Topo. e
L-CSMA	-268.5	-541.4	-190.8	-538.3	-1.8
Our Solution	-3.9	-2.8	-3.8	-3.5	-0.9

Fig. 5 shows the evolution of transmission aggressiveness r and number of connection n_s of topology a. We observe that by applying our solution, TA r and the number of connections n_s are stable. Note that dropping probability r of each link, around 0.001 ~ 0.003, is very small, so it does not waste too much bandwidth by dropping large number of packets. The number of connection n_s link 2 opens is around 15 in the simulation. The number of connections can be reduced by using a small k . Larger k ensures finer granularity in adjusting n_s , thus more responsive to the change in T_s , and therefore better system performance, but at the cost of consuming more device resources. In reality, both link backoff procedure and

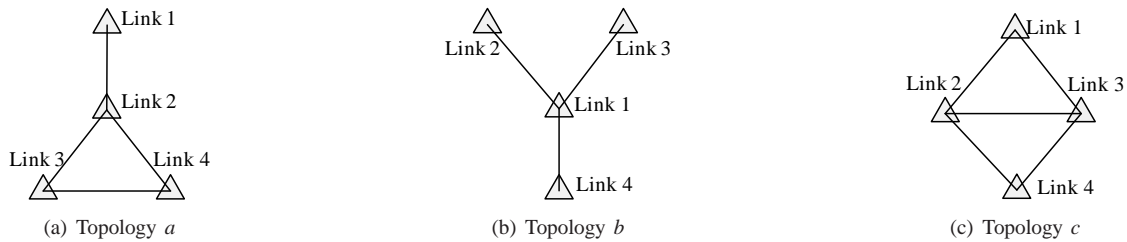


Fig. 3. Link Conflict Graphs of single-hop network topologies.

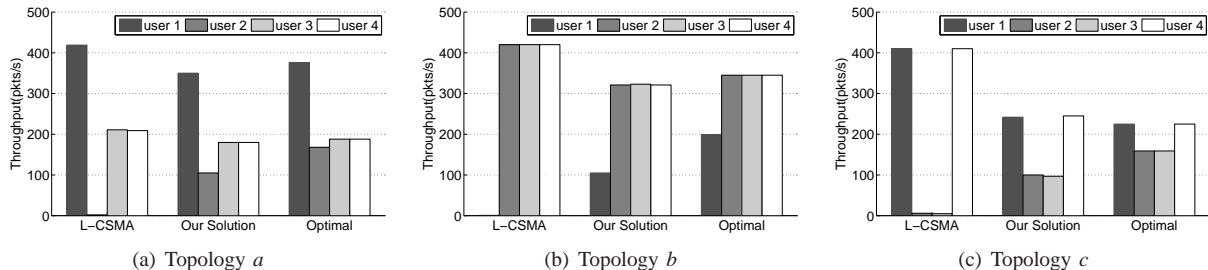


Fig. 4. Throughput under 1) L-CSMA: NS-2 simulation of TCP Reno over L-CSMA, 2) our solution: NS-2 simulation of multi-connection TCP Reno over A-CSMA with AQM and 3) optimal throughput computed from problem **MP**.

transmission delay affects RTT, result in very dynamic in RTT. This is why we see sharp oscillation of n_s in Fig. 5, because n_s is tuned to remove RTT bias. We can smooth the n_s by take the average of the current value and last value, but at the cost of not responsive to the change in T_s .

The results indicate that our multi-connection TCP Reno over A-CSMA with AQM scheme achieves the fair and efficient rate allocation among different users in the single hop scenario.

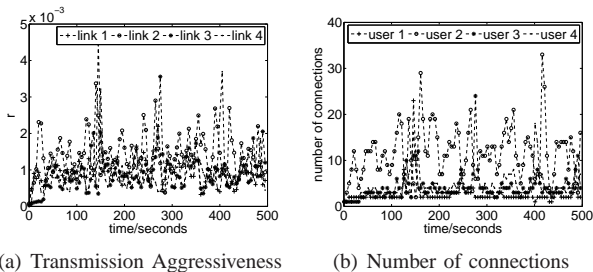


Fig. 5. Simulation results for topology *a* under multi-connection TCP Reno over A-CSMA with AQM: curves of transmission aggressiveness and number of connections.

B. Multihop Networks Scenario

In this part, we consider multiple hop networks scenario. The simulated topology and its associated conflict graph under study is shown in Fig. 6(a). It is a nine-node wireless network with two wireless APs denoted by node *d* and node *h*. Wireless client nodes *a*, *b* and *c* are associated with AP *d* while wireless client node *i* is associated with AP *h*. Nodes *e*, *f* and *g* are wired nodes. In the graph, wireless links are represented by dashed line and wired links are represented by solid line. There are three user flows whose paths are from node *a* to node *g*, node *b* to node *c* and node *i* to *g* respectively. The wired link *f*-to-*g* has the link capacity of 2Mb and other wired links have the link capacity of 20 Mb. So the wired bottleneck is on the link *f*-to-*g*. The wireless link bandwidth is 11 Mb. Other simulation parameters are the same as the previous simulations.

Fig. 6(b) plots the optimal throughput and throughput achieved by multi-connection TCP Reno scheme and TCP Reno over L-CSMA. The middle TCP flow starves when running TCP Reno over L-CSMA. In contrast, multi-connection TCP Reno over A-CSMA with AQM scheme assigns 83 packets to middle TCP flow, which is within 25% of the optimal achievable rate for this topology.

Fig. 6(c) and 6(d) give the evolution of transmission aggressiveness r and number of connection n_s . They are both stable in this scenario. The r is mostly around 0.003, therefore, the dropping probability is not large.

The results indicate that our multi-connection TCP over A-CSMA with AQM scheme is also applicable for multiple hop networks scenario.

C. Multihop Networks with Wireless and Wired Links Scenario

In this subsection, we validate our multi-connection TCP Reno solution for multihop networks with wired and wireless links scenario. The simulated topology under study is shown in Fig. 7(a). It is a nine-node wireless network with two wireless APs denoted by node *d* and node *h*. Wireless client nodes *a*, *b* and *c* are associated with AP *d* while wireless client node *i* is associated with AP *h*. Nodes *e*, *f* and *g* are wired nodes. In the graph, wireless links are represented by dashed line and wired links are represented by solid line. There are three user flows whose paths are from node *a* to node *g*, node *b* to node *c* and node *i* to *g* respectively. The wired link *f*-to-*g* has the link capacity of 2Mb and other wired links have the link capacity of 20 Mb. So the wired bottleneck is on the link *f*-to-*g*. The wireless link bandwidth is 11 Mb. Other simulation parameters are the same as the previous simulations.

Fig. 7(b) plots the simulation throughput and optimal throughput. We observe TCP Reno does not suffer server starvation over L-CSMA in this topology. However, the utility gap of our solution is -0.9 which is closer to zero than that of TCP Reno over L-CSMA, whose utility gap is -1.8 . This result validates our solution has better performance than that of TCP Reno over L-CSMA. The results validate multi-connection TCP Reno can work properly in multihop networks with wired and wireless links.

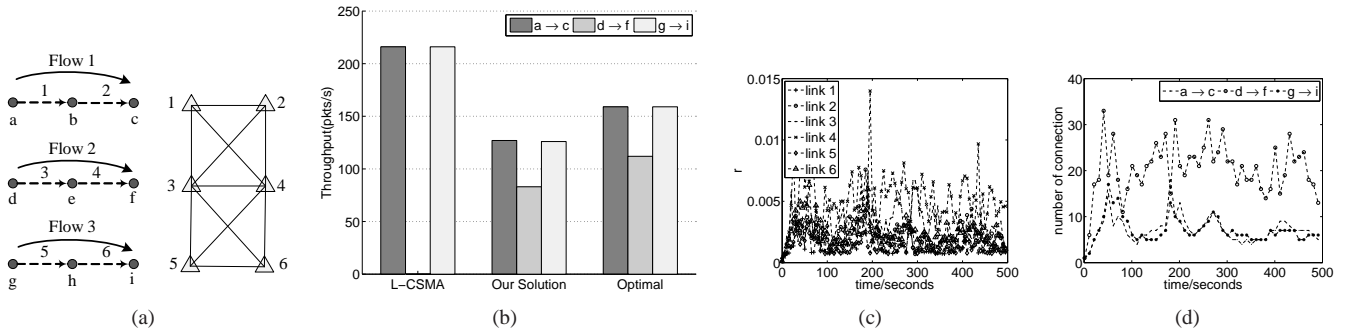


Fig. 6. Multihop networks scenarios: (a) topology d and its associated conflict graph. (b) throughput (c) curves of transmission aggressiveness. (d) curves of number of connections.

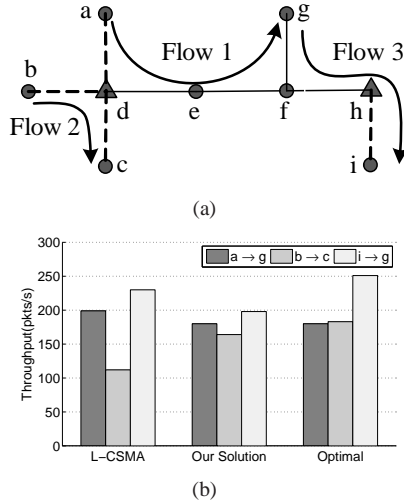


Fig. 7. Multihop networks with wired and wireless links scenario: (a) topology e (b) throughput

VII. CONCLUSION

In this paper, we study whether the widely-installed TCP Reno is compatible with adaptive CSMA. We find that running TCP Reno directly over adaptive CSMA suffers from the same severe starvation problems as TCP Reno over legacy CSMA (IEEE 802.11). The reason the potentials of adaptive CSMA cannot be realized by TCP Reno is that the overall system is not stable.

We then propose a multi-connection TCP Reno solution to inter-work with A-CSMA in a compatible manner. By adjusting the number of TCP connections for each session, our solution can achieve arbitrary system utility.

Our solution can be implemented at the application layer or transport layer. Application layer implementation requires no kernel modification, and the solution can be readily deployed in networks running adaptive CSMA. Finally, we show that our solution is applicable to single-hop wireless networks as well as multihop networks with wired and wireless links.

REFERENCES

- [1] X. Wang and K. Kar, "Throughput modelling and fairness issues in CSMA/CA based ad-hoc networks," in *Proceedings of IEEE INFOCOM*, 2005.
- [2] S. Liew, C. Kai, J. Leung, and B. Wong, "Back-of-the-envelope computation of throughput distributions in CSMA wireless networks," *IEEE Trans Mobile Computing*, 2010. [Online]. Available: <http://arxiv.org/pdf/0712.1854>
- [3] L. Jiang and J. Walrand, "A distributed CSMA algorithm for throughput and utility maximization in wireless networks," in *Proceedings of Communication, Control, and Computing*, 2008, pp. 1511–1519.
- [4] J. Liu, Y. Yi, A. Proutiere, M. Chiang, and H. Poor, "Towards utility-optimal random access without message passing," *Wireless Communications and Mobile Computing*, pp. 115–128, 2010.
- [5] J. Ni, B. Tan, and R. Srikant, "Q-CSMA: Queue-Length based CSMA/CA algorithms for achieving maximum throughput and low delay in wireless networks," in *IEEE INFOCOM Mini-Conference*, 2010.
- [6] S. Rajagopalan and D. Shah, "Distributed algorithm and reversible network," in *Proceedings of CISS*, 2008, pp. 498–502.
- [7] M. Chen, S. Liew, Z. Shao, and C. Kai, "Markov approximation for combinatorial network optimization," in *Proceedings of IEEE INFOCOM*, 2010.
- [8] J. Lee, J. Lee, Y. Yi, S. Chong, A. Proutiere, and M. Chiang, "Implementing Utility-Optimal CSMA," in *Proceedings of Allerton Conference*. Citeseer, 2009.
- [9] S. Rangwala, A. Jindal, K. Jang, K. Psounis, and R. Govindan, "Neighborhood-centric congestion control for multi-hop wireless mesh networks," *IEEE/ACM Transactions on Networking*, 2009.
- [10] K. Tan, F. Jiang, Q. Zhang, and X. Shen, "Congestion control in multihop wireless networks," *IEEE Transactions on Vehicular Technology*, pp. 863–873, 2007.
- [11] M. Chen and A. Zakhor, "Flow control over wireless network and application layer implementation," in *Proceedings of IEEE INFOCOM*, 2006.
- [12] S. Tullimas, T. Nguyen, R. Edgecomb, and S. Cheung, "Multimedia streaming using multiple TCP connections," *ACM TOMCCAP*, pp. 1–20, 2008.
- [13] X. Lin and N. Shroff, "Joint rate control and scheduling in multihop wireless networks," in *IEEE CDC*, 2004.
- [14] L. Chen, S. Low, and J. Doyle, "Joint congestion control and media access control design for ad hoc wireless networks," in *Proceedings of IEEE INFOCOM*, 2005.
- [15] M. Chen and A. Zakhor, "Multiple TFRC connections based rate control for wireless networks," *IEEE Transactions on Multimedia*, pp. 1045–1062, 2006.
- [16] S. Floyd and V. Jacobson, "Random early detection gateways for congestion control," *IEEE/ACM Transactions on Networking*, pp. 397–412, 1993.
- [17] D. Clark and W. Fang, "Explicit allocation of best-effort packet delivery service," *IEEE/ACM Transactions on Networking*, pp. 362–373, 1998.
- [18] L. Jiang and S. Liew, "Improving throughput and fairness by reducing exposed and hidden nodes in 802.11 networks," *IEEE Transactions on Mobile Computing*, pp. 34–49, 2008.
- [19] C. Chau, M. Chen, and S. Liew, "Capacity of large-scale CSMA wireless networks," in *Proceedings of MobiCom*, 2009, pp. 97–108.
- [20] K. Jain, J. Padhye, V. Padmanabhan, and L. Qiu, "Impact of interference on multi-hop wireless network performance," *Wireless Networks*, pp. 471–487, 2005.
- [21] B. Baker, "Approximation algorithms for np-complete problems on planar graphs," *Journal of the ACM*, pp. 153–180, 1994.
- [22] R. Boorstyn, A. Kershbaum, B. Maglaris, and V. Sahin, "Throughput

analysis in multihop CSMA packet radio networks,” *IEEE Transactions on Communications*, pp. 267–274, 1987.

- [23] S. Shakkottai and R. Srikant, “Network optimization and control,” in *Foundations and Trends in Networking*, 2007, pp. 271–379.
- [24] A. Tang, J. Wang, S. Low, and M. Chiang, “Equilibrium of heterogeneous congestion control: Existence and uniqueness,” *IEEE/ACM Transactions on Networking*, p. 837, 2007.
- [25] J. Mo and J. Walrand, “Fair end-to-end window-based congestion control,” *IEEE/ACM Transactions on Networking*, pp. 556–567, 2000.
- [26] L. Jiang and J. Walrand, “Convergence and stability of a distributed CSMA algorithm for maximal network throughput,” *UC Berkeley, Mar*, pp. 2009–43, 2009.
- [27] Z. Shao, M. Chen, A. S. Avestimehr, and S. Li, “Cross-layer Optimization for Wireless Networks with Deterministic Channel Models,” in *Proceedings of IEEE INFOCOM*, 2010.

APPENDIX

A. Starvation of TCP Reno over L-CSMA

We will explain why starvation happens in L-CSMA (CSMA/CA) networks. In L-CSMA (IEEE 802.11), all link has equal transmission aggressiveness r_l . Hence, for simplicity, we define $\rho = \exp(\beta r_l)$. From (3), the link throughput achieved by L-CSMA is then given by

$$y_l = \frac{\sum_{i:l \in \mathcal{I}_i} (\prod_{l \in \mathcal{I}_i} \rho)}{\sum_{i \in \mathcal{I}} (\prod_{l \in \mathcal{I}_i} \rho)}, \quad \forall l \in E. \quad (27)$$

As seen from (27), L-CSMA only can schedule a small fraction of capacity region, and is therefore not throughput-optimal.

We use a simple example to illustrate the starvation of TCP over CSMA/CS networks and explain why this problem remains unsolved. Fairness is one of the key problems that must be considered in designing any MAC, which allows contending links to share the wireless channel fairly. The random backoff algorithm in the L-CSMA network gives each host equal average count-down counter to grab the channel during transmission. This random count-down algorithm works fine in a symmetric environment where all hosts connected to a single access point. However, in asymmetric settings, it fails to achieve the fair channel accessing. Even though a fair higher layer rate control protocol such as TCP cannot solve this MAC layer fairness problem.

Consider the example shown in Fig. 1(a), where each of the four links runs L-CSMA MAC algorithm. The left hand side figure shows four nearby WLANs, whose access points denoted by triangle each connects to a single wireless client denoted by a circle. The right hand side figure gives the conflict graph of the networks. There is one TCP Reno session running over each link. This network topology is first studied in [2]. We run NS2 simulations to study the rate of each TCP Reno flows. The data rate of L-CSMA is 11Mbps and packet payload is 1000Bytes in simulation. Simulation results show that rate of link 2 is nearly zero, while rates of other links get higher rates.

This starvation is caused by the fundamental inefficiency of L-CSMA, and can be intuitively explained as follows. When link 1 is transmitting, link 2 will freeze its count down process because it is within the carrier sensing range of link 1. While link 2 is frozen, either link 3 or link 4 can transmit. This will continuously freeze link 2 after link 1 finishes its transmission. Link 1, link 3 and 4 take turns to occupy the channel, leaving link 2 very small chance to transmit.

In particular, the independent sets for the example in Fig.1(a) are $\emptyset, \{1\}, \{2\}, \{3\}, \{4\}, \{1, 3\}, \{1, 4\}$, and link 2’s throughput can be computed by (27) as follows

$$y_2 = \frac{\rho}{2\rho^2 + 4\rho + 1}. \quad (28)$$

where $\rho \approx 2.24$ for networks running L-CSMA under practical setting [1]. Plugging ρ into (28), we observe that $y_2 \approx 0.11$, which is much smaller compared to the throughput of other links. As such, the TCP Reno session running over link 2 starves. For more discussions on the starvation of TCP Reno over L-CSMA, please refer to [1] [2] [9] [10].

B. TCP Reno over A-CSMA with AQM

In this solution, the only modification needed is each transmitter of link l applies an AQM policy that each link drops the incoming packet with probability proportional to r_l .

1) *TCP Reno starves*: We conduct an NS-2 simulation to demonstrate the problem. The simulation topology and setup are the same as that in Fig. 1(a). But each link l drops incoming packets with probability proportional to r_l . We also give the backward links higher priority. The simulation results are shown in Fig. 8(a), from which we can see that user 2 starves. Fig. 8(b) and 8(c) show the transmission aggressiveness of the links, and RTT of TCP Reno sessions, respectively. We observe that all links have closely equal transmission aggressiveness. Under this situation, by now it should be clear that link 2 will starve.

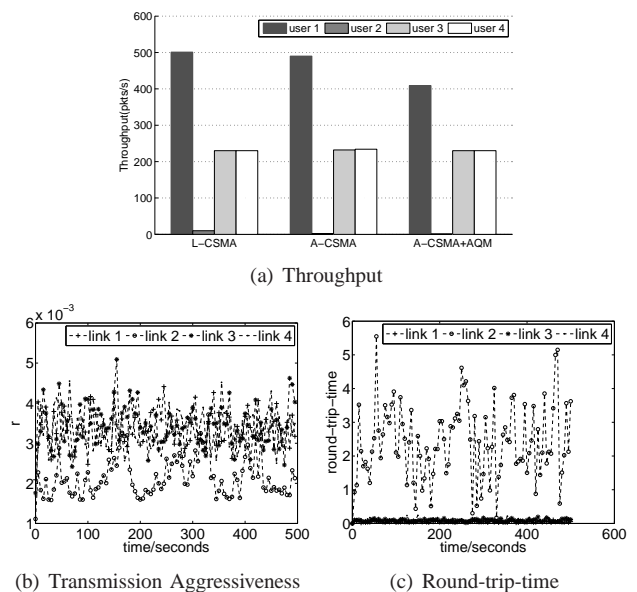


Fig. 8. Simulation Results: TCP Reno over A-CSMA with AQM.

2) *Explanation*: We present the analysis as follows. In this example, there are four TCP Reno sessions $s = 1, 2, 3, 4$, each running over a wireless link $l = 1, 2, 3, 4$. With TCP Reno as

the rate control algorithm, the algorithms in (9)-(10) turn into:

$$\begin{cases} \dot{x}_s = \frac{x_s^2}{2} \left(\frac{2}{T_s^2 x_s^2} - r_s \right)_{x_s}^+, \quad \forall s = 1, 2, 3, 4; & (29) \\ \dot{r}_s = \alpha [x_s - \sum_{i:s \in i} \tau_i(\mathbf{r})]_{r_s}^+, \quad \forall s = 1, 2, 3, 4; & (30) \\ \tau_i(\mathbf{r}) = \frac{\exp(\sum_{s \in i} \beta r_s)}{\sum_{i' \in \mathcal{I}} \exp(\sum_{s \in i'} \beta r_s)}, \quad \forall i \in \mathcal{I}; & (31) \\ T_s = \frac{1}{\alpha} \frac{r_s}{x_s}, \quad \forall s = 1, 2, 3, 4. & (32) \end{cases}$$

The first equation is the TCP Reno updating equation, as discussed in (6). The second and the third equations correspond to A-CSMA scheduling and the transmission aggressiveness adjusting equation.

The fourth equation characterizes the RTT user s experiences. As we mentioned in the simulation settings, to simplify the analysis, we only consider the forward link by giving the TCP ACK higher priority to transmit. Therefore, the waiting time of TCP ACK is very short. Most of the packets are buffered at the queue of forward link. Thus, $W_s \approx Q_s$ (recall W_s is the congestion window size of TCP Reno session of user s), and round trip time T_s can be written as

$$T_s = \frac{W_s}{x_s} \approx \frac{Q_s}{x_s}, \quad (33)$$

where Q_s is the queue length of link s used by user s . According to A-CSMA, the transmission aggressiveness is proportional to the queue length. Thus we obtain (32):

$$T_s = \frac{Q_s}{x_s} = \frac{1}{\alpha} \frac{r_s}{x_s}, \quad \forall s = 1, 2, 3, 4. \quad (34)$$

Note the algorithms in (29)-(32) are a special case of the generic one in (9)-(10), except the last RTT equation in (32). The RTT equation reveals a subtle interaction between TCP Reno and A-CSMA, which in fact causes the starvation. We explain it as below.

At the equilibrium of the dynamic system described in (29)-(32), the derivatives are all zero. Hence,

$$r_s = \frac{2}{T_s^2 x_s^2}, \quad \forall s = 1, 2, 3, 4. \quad (35)$$

Solving (34) and (35), we arrive at the following observations:

$$r_s = 2^{1/3} \alpha^{2/3}, \quad \forall s = 1, 2, 3, 4. \quad (36)$$

Thus every link s has the same r_s and competes the channel with the same level of transmission aggressiveness. Under this situation, our previous discussions indicate that links 1, 3 and 4 will take turns to freeze link 2, and hence the TCP Reno over link 2 will starve.

C. Proof to Theorem 2

We give the proof of Theorem 2 as follows:

Proof: 1) By relaxing the first set of inequalities (15) of problem **MP**, we get its partial Lagrangian as follows:

$$L(\mathbf{x}, \boldsymbol{\tau}, \mathbf{r}) = \sum_{s \in \mathcal{S}} U_s(x_s) - \frac{1}{\beta} \sum_{i \in \mathcal{I}} \tau_i \log \tau_i - \sum_{l \in E} r_l \left(\sum_{s: l \in s, s \in \mathcal{S}} x_s - \sum_{i: l \in i} \tau_i \right), \quad (37)$$

where $\mathbf{r} = [r_l, l \in E]$ is the vector of Lagrange multipliers. We notice that $\sum_{l \in E} r_l \sum_{i: l \in i} \tau_i = \sum_{i \in \mathcal{I}} \tau_i \sum_{l \in i} r_l$. Since the problem

MP is a concave optimization problem and Slater's condition holds, the optimal solution of problem **MP** can be found by solving the following problem successively in $\boldsymbol{\tau}$, \mathbf{x} and \mathbf{r} :

$$\begin{aligned} \min_{\mathbf{r} \geq 0} \max_{\mathbf{x} \geq 0, \boldsymbol{\tau} \geq 0} & \sum_{s \in \mathcal{S}} U_s(x_s) - \sum_{l \in E} r_l \sum_{s: l \in s} x_s \\ & + \sum_{i \in \mathcal{I}} \tau_i \sum_{l \in i} r_l - \frac{1}{\beta} \sum_{i \in \mathcal{I}} \tau_i \log \tau_i \\ \text{s.t.} & \sum_{i \in \mathcal{I}} \tau_i = 1. \end{aligned} \quad (38)$$

Define

$$g_\beta(\mathbf{r}) \triangleq \frac{1}{\beta} \log \left(\sum_{i \in \mathcal{I}} \exp(\beta \sum_{l \in i} r_l) \right). \quad (39)$$

The conjugate of $g_\beta(\mathbf{y})$ is defined as $g^*(z) = \sup_{\mathbf{y} \in \text{dom} g} (z^T \mathbf{y} - g(\mathbf{y}))$. Therefore, the conjugate of $g_\beta(\mathbf{r})$ is given by

$$g_\beta^*(\boldsymbol{\tau}) = \begin{cases} \frac{1}{\beta} \sum_{i \in \mathcal{I}} \tau_i \log \tau_i & \text{if } \boldsymbol{\tau} \geq 0 \text{ and } 1^T \boldsymbol{\tau} = 1 \\ \infty & \text{otherwise.} \end{cases} \quad (40)$$

The conjugate of its conjugate is itself, i.e., $g_\beta(\mathbf{r}) = g_\beta^{**}(\mathbf{r})$. Therefore, we have

$$\begin{aligned} g_\beta(\mathbf{r}) &= \max_{\boldsymbol{\tau} \geq 0} \sum_{i \in \mathcal{I}} \tau_i \sum_{l \in i} r_l - \frac{1}{\beta} \sum_{i \in \mathcal{I}} \tau_i \log \tau_i \\ \text{s.t.} & \sum_{i \in \mathcal{I}} \tau_i = 1, \end{aligned} \quad (42)$$

with the corresponding unique optimal solution

$$\tau_i(\mathbf{r}) = \frac{\exp(\sum_{l \in i} \beta r_l)}{\sum_{i' \in \mathcal{I}} \exp(\sum_{l \in i'} \beta r_l)}, \quad \forall i \in \mathcal{I}. \quad (43)$$

(Note this is the exact stationary distribution that CSMA Markov chain achieves. Hence, A-CSMA can be used to solve this subproblem.) From (39) and (42), formula (38) will be

$$\begin{aligned} \min_{\mathbf{r} \geq 0} \max_{\mathbf{x} \geq 0} & \sum_{s \in \mathcal{S}} U_s(x_s) - \sum_{l \in E} r_l \sum_{s: l \in s} x_s \\ & + \frac{1}{\beta} \log \left(\sum_{i \in \mathcal{I}} \exp(\beta \sum_{l \in i} r_l) \right). \end{aligned} \quad (44)$$

Define

$$L_2(\mathbf{x}, \mathbf{r}) \triangleq \sum_{s \in \mathcal{S}} U_s(x_s) - \sum_{l \in E} r_l \sum_{s: l \in s} x_s + \frac{1}{\beta} \log \left(\sum_{i \in \mathcal{I}} \exp(\beta \sum_{l \in i} r_l) \right). \quad (45)$$

The saddle point of above formula is the optimal primal and dual variable. Therefore, the partial derivative is equal to zero, we have

$$\frac{\partial L_2(\mathbf{x}, \mathbf{r})}{\partial x_s} = U'_s(x_s) - \sum_{l \in s} r_l = 0, \quad (46)$$

$$\frac{\partial L_2(\mathbf{x}, \mathbf{r})}{\partial r_l} = -r_l \left(\sum_{s: l \in s} x_s - \sum_{i: l \in i} \tau_i(\mathbf{r}) \right) = 0. \quad (47)$$

When $U_s(x_s) = \frac{1}{x_s}$, a primal-dual algorithm that solves above problem is

$$\begin{cases} \dot{x}_s = f(x_s) \left(\frac{2n_s^2}{T_s^2 x_s^2} - \sum_{l \in s} r_l \right)_{x_s}^+, \quad \forall s \in \mathcal{S}; & (48) \\ \dot{r}_l = \alpha(r_l) \left[\sum_{s: l \in s} x_s - \sum_{i: l \in i} \tau_i(\mathbf{r}) \right]_{r_l}^+, \quad \forall l \in L. & (49) \end{cases}$$

Plus the (43), we now have that the equilibrium of dynamic system in (8)-(10) solves **MP**.

2) The proof can use the same set of standard Lyapunov elaborated in [7].